JOC The Journal of Organic Chemistry

Article

pubs.acs.org/joc

Synthesis and Optoelectronic Properties of 6,12-Bis(amino)anthanthrene Derivatives

Jean-Benoît Giguère and Jean-François Morin*

Département de Chimie and Centre de Recherche sur les Matériaux Avancés (CERMA), Université Laval, 1045 Ave de la Médecine, Québec, Canada G1V 0A6

Supporting Information

ABSTRACT: A series of 6,12-bis(amino) anthanthrene-based conjugated molecules were prepared and characterized using UV−vis and fluorescence spectroscopy and cyclic voltammetry. The absorption spectra and redox potentials of these molecules can be modulated by changing the conjugated moieties linked at the 4 and 10 positions. Moreover, the optoelectronic properties of these derivatives strongly depend on the moieties attached to the nitrogen atoms at the 6 and 12 positions.

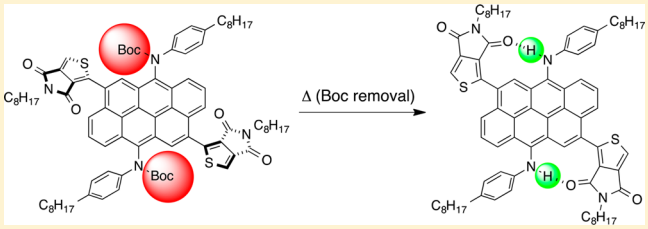

INTRODUCTION

π-Conjugated organic semiconductors have become valuable materials for numerous applications ranging from bioimaging[1] to organic electronics[2] because of their easily tunable optoelectronic properties. Depending on different structural and electronic features such as the effective conjugation length, the overlap between π orbitals, and the presence of electron-withdrawing (EW) and/or electron-donating (ED) groups, it is possible to access a wide range of optical and electronic properties. Moreover, π-conjugated molecules can exhibit very good hole- and/or electron-transport properties in thin films while absorbing light over the visible/near-infrared spectrum.[2] The modulation of these properties is accessible through introduction of functional groups. For instance, ED and EW groups lead to good hole- and electron-transport properties, respectively, while a combination of both within the same molecule allows a significant reduction of the band gap, shifting the light absorption toward lower energy. Thus, several ED and EW functional groups have been developed in the past 20 years as they have proved to be the best instruments for the fine-tuning of electronic properties of conjugated molecules.[2]

Triarylamines (Ar_3N) are particularly interesting functional groups since they are redox-active and chemically versatile. Triarylamine moieties can be introduced in a molecule to provide hole-transporting properties[3] (low oxidation potential and reversible redox processes) or used in combination with an EW group in a donor−acceptor strategy to lower the electronic band gap. The latter strategy has been used several times by researchers in the photovoltaic area to prepare highly efficient materials whose absorption spectra in the solid state closely match the solar spectrum.[4−6] While the use of triarylamines is common in organic electronics, reports of molecules possessing secondary diarylamines (Ar_2NH) are much less abundant, and to our knowledge, no obvious reason explains such a stark difference in usage between the two parent structures. Diarylamines offer unexploited possibilities in terms of *N*-functionalization and intermolecular interactions (coordination chemistry, reduced steric hindrance, and hydrogen bonding) to further tailor the properties of the desired materials.[7] Recently, pigments of the well-known quinacridone family carrying a diarylamine motif were successfully used in organic field-effect transistors (OFETs) with hole mobilities of up to 0.2 $cm^2\ V^{-1}\ s^{-1}$ (1.5 $cm^2\ V^{-1}\ s^{-1}$ for epindolidione), taking advantage of the hydrogen-bonding capabilities of the secondary diarylamine structure in the control of intermolecular interactions and packing.[8] Moreover, *N*-alkylated heterocyclic compounds such as carbazole[9] and diketopyrrolopyrrole[10] have been extensively studied, probably because of the good interplay between solubility and desired properties.

We recently undertook the functionalization of the commercially available polycyclic pigment 4,10-dibromoanthanthrone (Vat Orange 3, compound **1** in Scheme 1).[11] The anthanthrone scaffold is a cheap and versatile polycyclic building block with two axes of functionalization: the bromines at the 4 and 10 positions and the ketones at the 6 and 12 positions. Because of their synthetic complexity, polycyclic aromatics with nonlinearly fused cycles have been less studied than their linear acene analogues, although they should offer highly desirable properties and possibly overcome some shortcomings, notably their sensitivity to oxidation.[12]

Herein we report the synthesis of 4,10-disubstituted 6,12-bis(imino)dihydroanthanthrene and 6,12-bis(amino)-anthanthrene compounds to study the effect of amine substitution on the optoelectronic properties of polycyclic π-conjugated molecules.[13] We sought to understand how the presence of a secondary amine at the 6 and 12 positions influences the solid-state packing of anthanthrene derivatives.

Received: October 22, 2013
Published: November 26, 2013

Scheme 1. Imine Condensation and Synthesis of the Starting Building Blocks Br-AA-NBoc and 2

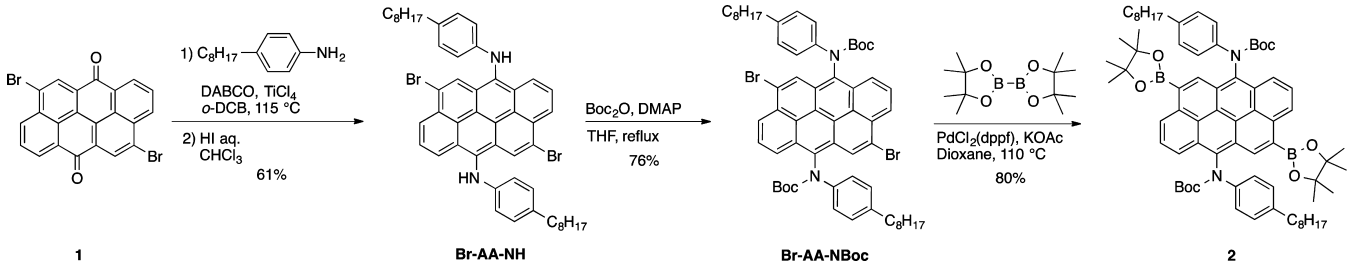

Scheme 2. Stille and Suzuki Couplings of Br-AA-NBoc and 2 with Different Aromatic Moieties and Subsequent *N*-Boc Thermal Deprotection

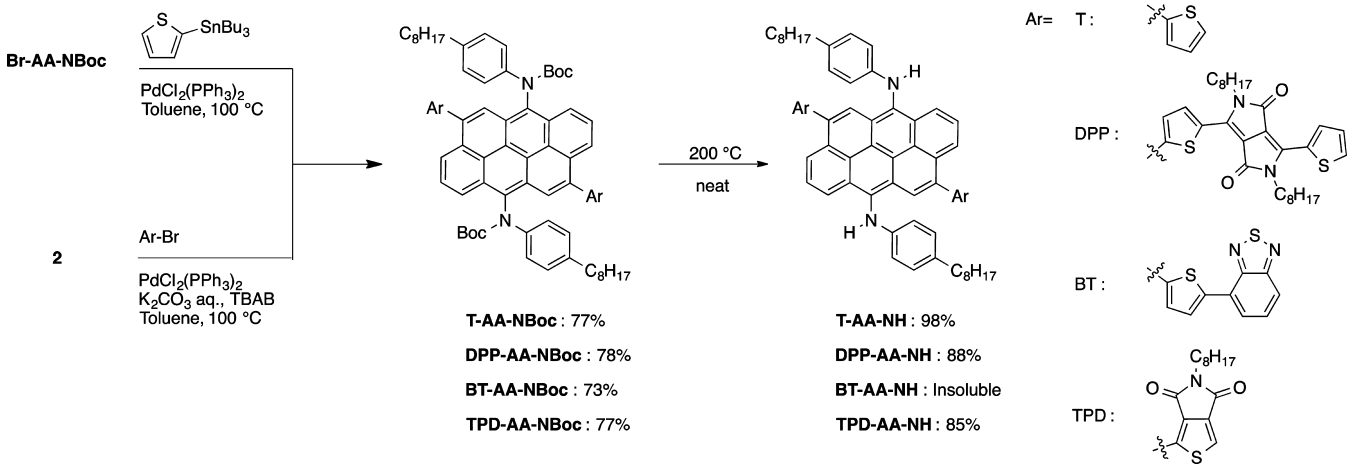

The 6,12-bis(amino)anthanthrene moiety is later termed anthanthramine (AA) for concision and clarity.

RESULTS AND DISCUSSION

Synthesis. 4,10-Dibromoanthanthrone (**1**) was used as the starting material for the $TiCl_4$-mediated imine condensation with 4-octylaniline (Scheme 1). The very low reactivity of acenequinones requires the use of a Lewis acid and a dehydratating agent, $TiCl_4$ in our case, for the reaction to take place. *o*-Dichlorobenzene was used as the solvent because of its high boiling point. The poorly soluble bisimine was obtained as a crude product and was subsequently reduced to the anthanthramine derivative (**Br-AA-NH**) using aqueous hydrogen iodide.[14] It is worth noticing that reduction with $NaBH_4$ proved unreliable, possibly because of the very low solubility of the starting material in THF. The secondary amines of compound **Br-AA-NH** were protected with *tert*-butyloxycarbonyl (Boc) groups for multiple reasons: (1) to improve the solubility, allowing easier characterization and purification; (2) to modulate the optoelectronic and packing properties; (3) to eliminate the possibility of Buchwald–Hartwig amination as a side reaction during palladium-catalyzed reactions, and (4) ease of deprotection using different methods. The *N*-Boc protection reaction was performed under classical conditions using DMAP as a catalyst, but to our surprise, we obtained compound **Br-AA-NBoc** as a mixture of what we believe to be *syn* and *anti* isomers. Both isomers were visible on silica TLC and caused a duplication of some peaks in the NMR spectrum (see Figure S2 in the Supporting Information). To further expand the scope of the anthanthramine moiety as a building block for π-conjugated materials, we prepared the bis(pinacolboronate) compound by reaction of **Br-AA-NBoc** with the corresponding diboron reagent under Miyaura borylation conditions[15] to afford compound **2** in good yield (Scheme 1).

Having the brominated and borylated building blocks in hands, we undertook the functionalization at the 4 and 10 positions with different conjugated units. These units were chosen according to their structural and electronic characteristics to study the effect of the extended π-conjugation on the modulation of the optoelectronic properties through donor–acceptor interactions. In some cases, thiophene units were used as linkers between the anthanthramine core and the conjugated units at the 4 and 10 positions to reduce the torsion angle, thus improving the conjugation.[16,17] We first prepared an electron-rich 2-thienylanthanthramine compound by using commercially available 2-(tributylstannyl)thiophene under Stille coupling conditions to afford **T-AA-NBoc** in 77% yield (Scheme 2).

Diketopyrrolopyrrole (**DPP**) was chosen because of its low band gap, moderate electron-withdrawing character, and high performance in organic electronics.[10] Both thieno[3,4-*c*]-pyrrole-4,6-dione (**TPD**) and benzothiadiazole (**BT**) are electron-withdrawing moieties and are widely used in organic solar cells (OSCs).[18] Furthermore, **TPD** offers the possibility of hydrogen bonding between the carbonyl and the amine as a driving force to push the planarization (vide infra, Figure 11). Monobromo-substituted conjugated moieties **DPP-Br**[19] and **TPD-Br**[20] were prepared according to published procedures, and **BT-Br** was prepared from 4-(2-thienyl)benzothiadiazole[21] via NBS bromination. The Suzuki couplings were performed under biphasic conditions using TBAB as a phase-transfer agent, and aryl-appended anthanthramines were obtained in 73–78% yield. It is important to note that all of the *N*-Boc compounds were highly soluble in common solvents.

dx.doi.org/10.1021/jo402313c | J. Org. Chem. 2013, 78, 12769–12778

Scheme 3. Imine Condensation with 4,10-Bis(4-octylthiophene)anthanthrone (3)

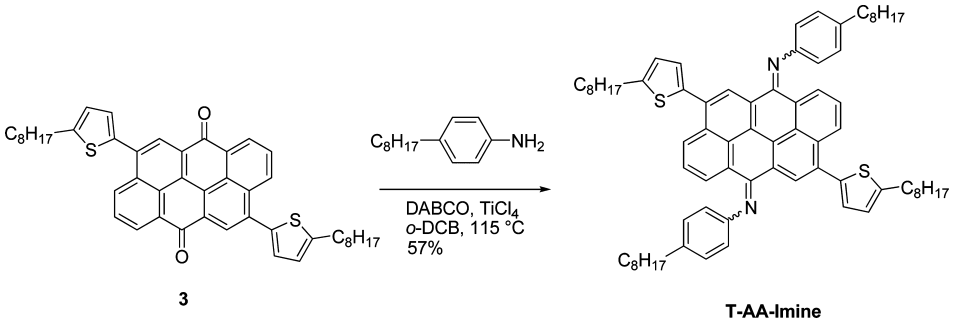

Table 1. Summary of the Optoelectronic Properties of Anthanthramine Compounds[a]

	optical properties				electrochemical properties				
compoud	λ_{max} (nm)	$E_g^{solution}$ (eV)	E_g^{film} (eV)	λ_{fluor} (nm)	V_{red} (V)	V_{ox} (V)	E_g (eV)	E_{HOMO} (eV)	E_{LUMO} (eV)
Br-AA-NH	480	2.28	2.07	578	−1.33	0.51	1.78	−5.18	−3.34
Br-AA-NBoc	457	2.62	2.51	464	−1.24	1.17	2.41	−5.84	−3.43
T-AA-NH	480	2.27	2.17	578	−1.45	0.40	1.85	−5.07	−3.22
T-AA-NBoc	463	2.57	2.53	484	electropolymerizes			–	–
DPP-AA-NH	568	2.00	1.77	-	−1.11	0.49	1.60	−5.16	−3.56
DPP-AA-NBoc	568	2.03	1.91	618	−1.07	0.87	1.94	−5.54	−3.60
BT-AA-NBoc	467	2.52	2.39	595	−1.30	0.99	2.29	−5.66	−3.37
TPD-AA-NH	493	2.20	1.99	607	−1.35	0.48	1.83	−5.15	−3.32
TPD-AA-NBoc	464	2.55	2.43	508	−1.23	1.07	2.30	−5.74	−3.44
T-AA-Imine	510	2.08	1.98	645	−1.01	1.03	2.04	−5.70	−3.66

[a] $E_g^{solution}$ and E_g^{film} were measured at the onset. *V* values are onsets vs Ag/AgCl at a scan rate of 100 mV s^{-1}. For Fc/Fc^+, $E_{1/2}$ was measured at 0.43 V vs Ag/AgCl. Vacuum levels were determined electrochemically with the Fc/Fc^+ level at 5.1 eV.

Deprotection of **DPP-AA-NBoc** using TFA in CH_2Cl_2 afforded poor conversion and led to significant amounts of side products. Instead, we opted for the reagent- and solvent-free thermal removal of the Boc groups.[22] The *N*-Boc thermal deprotection has the advantage of being amenable to solid-state postprocessing at moderate temperature in a functional device fabrication strategy.[21,23] The secondary diarylamine compounds were obtained in over 85% yield after the neat compound was heated at 200 °C accompanied by gas evolution (isobutylene, CO_2) and a visual bathochromic shift. The loss of the Boc groups reduced the solubility of the compounds to such an extent that **BT-AA-NH** was completely insoluble, making its characterization almost impossible. This decrease in solubility upon Boc removal is likely attributable to stronger intermolecular interactions through hydrogen bonding. It is interesting to note that the amine proton of **TPD-AA-NH** was shifted to lower field by almost 1 ppm (from ca. 6 to 7 ppm) relative to those of the other **AA-NH** compounds in the ^1H NMR spectrum. This is a clear indication of the presence of hydrogen bonding between the **TPD** carbonyl and the secondary amine proton (see Figure 11).

The imine function is of interest in organic electronics, where it generally acts as an electron-withdrawing moiety, as it allows the modulation of the optoelectronic properties[24] while keeping the quinoidal structure of the anthanthrone intact. Compound **T-AA-Imine** was prepared under the same condensation conditions as for compound **1** but using 5-octylthiophene-appended compound **3**[11] in order to obtain a more soluble compound (Scheme 3). The use of a thiophene-appended anthanthrone derivative also allowed the effect of intramolecular charge transfer between the electron-donating thiophene and electron-withdrawing imine to be studied. Compound **T-AA-Imine** was obtained in 57% yield as a mixture of the three possible isomers (two *syn*, one *anti*).

Optical Properties. The UV−vis and fluorescence spectra of selected compounds were recorded at concentrations of 10−50 μM with an excitation wavelength of λ_{max} − 30 nm. The results are reported as normalized spectra, and a summary of the optical properties is reported in Table 1.

The unsubstituted diarylamines **Br-AA-NH** and **Br-AA-NBoc** showed interesting spectral features. The introduction of the *N*-Boc group has a dramatic effect on the optical properties. The secondary amine **Br-AA-NH** has a broad absorption with a maximum (λ_{max}) at 480 nm, whereas **Br-AA-NBoc** presents a fine vibronic structure with λ_{max} blue-shifted to 457 nm (Figure 1). The most notable difference between the two compounds appeared in the solid state: **Br-AA-NH** has a band gap of 2.07 eV, which is 0.44 eV smaller than that of **Br-AA-NBoc** (2.51 eV). Moreover, **Br-AA-NBoc** presents a small Stokes shift of 7 nm, as opposed to the large Stokes shift of 98 nm for **Br-AA-NH**. The extensive differences in optical properties are caused by a combination of electronic and structural effects. In fact, the carbamate group has an electron-withdrawing carbonyl group that reduces the electron-donor character of the amine. Moreover, the bulkiness of the *N*-Boc group limits the rotational freedom, as evidenced by the presence of isomers, which makes the molecule more rigid and causes the appearance of a vibronic structure. The *N*-Boc group also limits the electron-donating character of the amine via resonance because Boc inhibits the formation of the conjugated planar sp^2-hybridized structure. In the solid state, the Boc groups hinder the intermolecular interactions in a face-to-face manner, which allows close $\pi-\pi$ interactions and lowers the band gap.

dx.doi.org/10.1021/jo402313c | J. Org. Chem. 2013, 78, 12769−12778

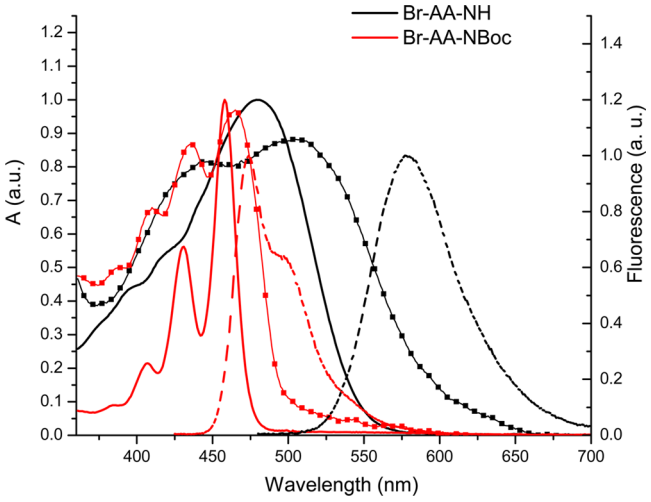

Figure 1. UV−vis spectra ($CHCl_3$, solid lines; thin films, square symbols) and fluorescence spectra ($CHCl_3$, dashed lines) of **Br-AA-NH** (black lines) and **Br-AA-NBoc** (red lines).

Thiophene-appended **T-AA-NH** and **T-AA-NBoc** have spectral features similar to those of the brominated analogues, with red shifts of less than 5 nm. Their spectra are presented in Figure S1 in the Supporting Information. The small red shift is indicative of the weak effect of the electron-donating moieties at the 4 and 10 positions on the optical properties, even though it extends the overall conjugated length. This result also suggests that the 4,10 conjugation axis might not be the best for the modulation of the electronic properties of anthanthramine derivatives.

The introduction of the low-band-gap diketopyrrolopyrrole moieties at the 4 and 10 positions causes a red shift of λ_{max} to 568 nm for both **DPP-AA-NH** and **DPP-AA-NBoc**. These two compounds present very similar absorption spectra in solution (Figure 2), and the band gap of **DPP-AA-NH** is lowered by 0.27 eV relative to **T-AA-NH**. This decrease is fairly small considering the electron-withdrawing character of the diketopyrrolopyrrole core and the extended conjugation. The absorption spectrum of **DPP-AA-NH** is very similar to that

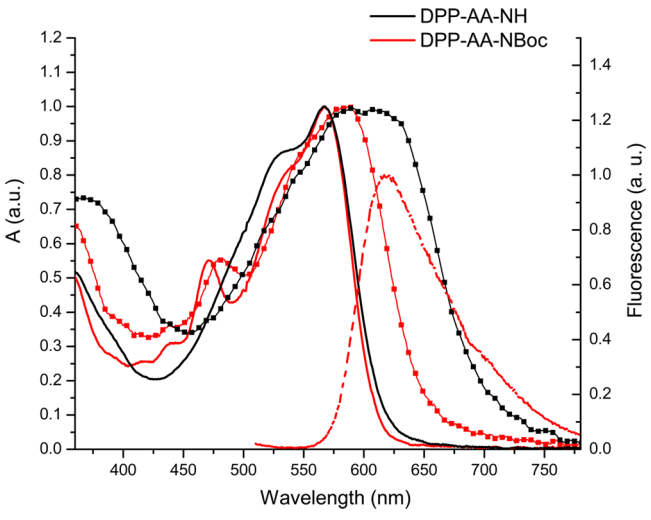

Figure 2. UV−vis spectra ($CHCl_3$, solid lines; thin films, square symbols) and fluorescence spectra ($CHCl_3$, dashed lines) of **DPP-AA-NH** (black lines) and **DPP-AA-NBoc** (red lines).

of the unsubstituted **DPP** moiety (λ_{max} = 552 nm),[25] indicating that the electronic communication between the two units in the ground state is rather limited (vide infra). Going from solution to the solid state, the absorption onset of **DPP-AA-NH** is red-shifted to 701 nm, possibly because of intermolecular interactions between the **DPP** and the electron-rich anthanthramine moiety.[25] The **DPP-AA-NH** fluorescence in solution is completely quenched, whereas **DPP-AA-NBoc** is weakly emissive with a moderate Stokes shift of 50 nm. It is reasonable to think that fluorescence quenching of **DPP-AA-NH** occurs via through-space electron or energy transfer between the anthanthramine and the electron-accepting **DPP**, as no charge-transfer band is observed in the absorption spectrum.

The **TPD-AA-NBoc** and **BT-AA-NBoc** analogues show very similar UV−vis spectra and a very limited red shift of less than 4 nm compared with **T-AA-NBoc** (Figure 3). The major

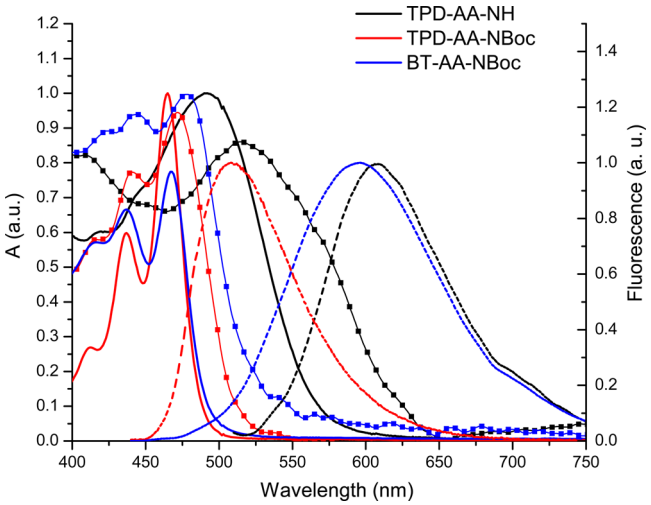

Figure 3. UV−vis spectra ($CHCl_3$, solid lines; thin films, square symbols) and fluorescence spectra ($CHCl_3$, dashed lines) of **TPD-AA-NH** (black lines), **TPD-AA-NBoc** (red lines), and **BT-AA-NBoc** (blue lines).

difference between the two species lies in their fluorescence spectra: the Stokes shift of the **BT** compound is much larger than that of the **TPD** analogue (128 vs 44 nm). The λ_{max} of **TPD-AA-NH** is slightly red-shifted by 13 nm to 493 nm versus **T-AA-NH** and follows the same trend as the **DPP**-appended compounds with a negligible electronic interaction between the electron-withdrawing moiety and the anthanthramine core.

T-AA-Imine has the same quinoidal structure as the anthanthrone starting material and presents a spectrum very similar to that of **3**[11] with a broad λ_{max} at 510 nm and a large fluorescence Stokes shift of 135 nm (Figure 4). The slight red shift of the absorption band in the solid state compared with solution (627 vs 596 nm) is indicative weak intermolecular interactions in the solid state. Even though the electronic communication between the anthanthramine core and the appended unit is limited, the use of the secondary diarylamine allows the control of the solid-state absorption spectrum toward lower energies, which is desirable for solar cell applications.

Solution Aggregation. In order to assess the aggregation behavior of anthanthramine compounds, the absorption spectra of **Br-AA-NH** in 3.0×10^{-5} M solutions with different chloroform/methanol solvent ratios were recorded (Figure 5).

dx.doi.org/10.1021/jo402313c | J. Org. Chem. 2013, 78, 12769−12778

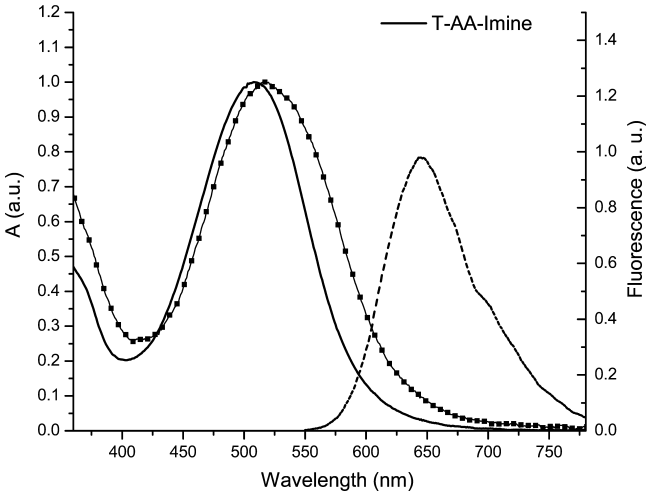

Figure 4. UV–vis spectra ($CHCl_3$, solid lines; thin films, square symbols) and fluorescence spectrum ($CHCl_3$, dashed line) of **T-AA-Imine**.

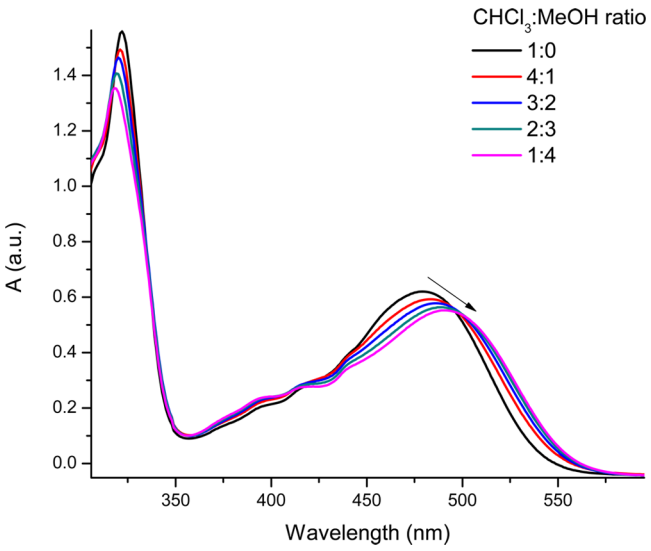

Figure 5. UV–vis spectra of **Br-AA-NH** at different $CHCl_3$/MeOH solvent ratios.

With increasing methanol content, a shift of the maximum was observed from 480 to 491 nm with an isosbestic point at 495 nm. The red shift is characteristic of J-aggregation as slipped face-to-face stacking.[26]

X-ray Diffraction. A thick film of **Br-AA-NBoc** was drop-casted on a glass slide from a 20 mg/mL $CHCl_3$ solution, and its XRD pattern (Figure 6) shows an amorphous structure with no long-range order and broad amorphous regions. Afterward, the thermal *N*-Boc deprotection was performed with the same sample by heating the glass slide on a hot plate at 200 °C in air for 20 min. The on-substrate deprotection induced long-range order for **Br-AA-NH** with new well-developed peaks and loss of the broad amorphous peaks. The interchain short-angle peak with a *d* spacing of 21.50 Å and a short $\pi-\pi$ distance, which can reasonably be assigned at d = 3.53 Å, were observed.

Electrochemistry. Electrochemical analysis allowed the determination of the redox potentials of the electro-active species and the determination of the positions of the HOMO and LUMO frontier orbitals. Cyclic voltammograms (CVs) were measured in CH_2Cl_2 with a $TBAPF_6$ electrolyte, platinum

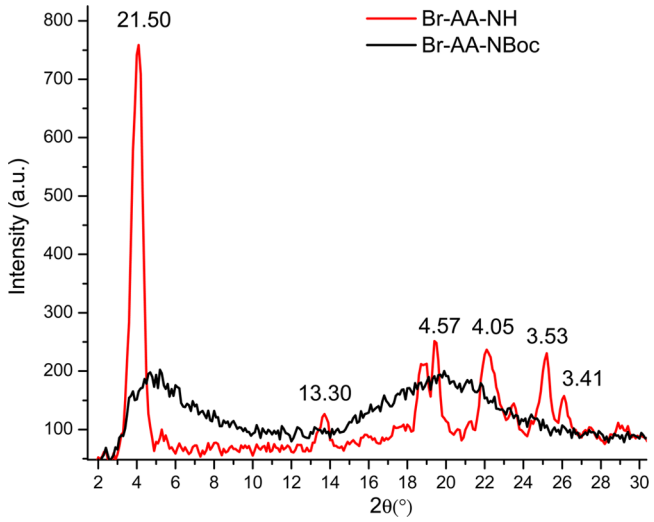

Figure 6. XRD profiles of **Br-AA-NBoc** (black line) and **Br-AA-NH** (red line) recorded as thick films on glass slides. *d* spacings in Å are specified over the corresponding peaks.

electrodes, and an Ag/AgCl reference electrode at a scan rate of 100 mV/s, and the potential values are reported at the onset of the current peak. The redox potentials and their corresponding HOMO and LUMO levels are reported in Table 1.

The difference between the oxidation potentials of **Br-AA-NH** and **Br-AA-NBoc** is quite large (Figure 7). In fact, removal

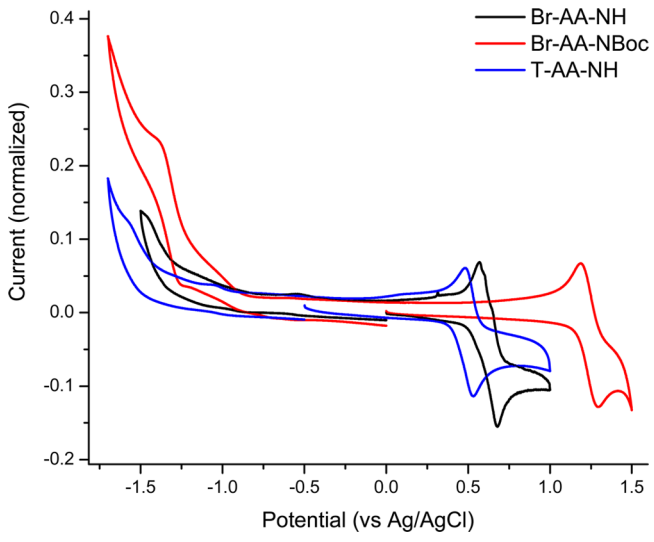

Figure 7. Cyclic voltammograms of the compounds **Br-AA-NH** (black line), **Br-AA-NBoc** (red line), and **T-AA-NH** (blue line).

of the *N*-Boc group reduces the oxidation potential by 0.66 V, from 1.17 to 0.51 V vs Ag/AgCl. Substitution with electron-donating thiophenes in **T-AA-NH** further reduces it by 0.11 V down to 0.40 V vs AgCl. Compound **T-AA-NBoc** presents a complex CV caused by electropolymerization at the electrode (not presented). Interestingly, the secondary amine in **T-AA-NH** offers enough stabilization to the radical cation so that electropolymerization is hindered. Electropolymerization followed by the *N*-Boc thermal deprotection could offer an interesting pathway to stable functionalized polymeric electrodes. This is in accordance with the lower optical band gap and

dx.doi.org/10.1021/jo402313c | J. Org. Chem. 2013, 78, 12769–12778

the stronger electron-donating character of the *N*-H group versus the *N*-Boc group.

Although **DPP-AA-NH** and **DPP-AA-NBoc** present the same reduction potential (ca. −1.10 V vs Ag/AgCl), their CVs are very different in the anodic region (Figure 8). Not only is

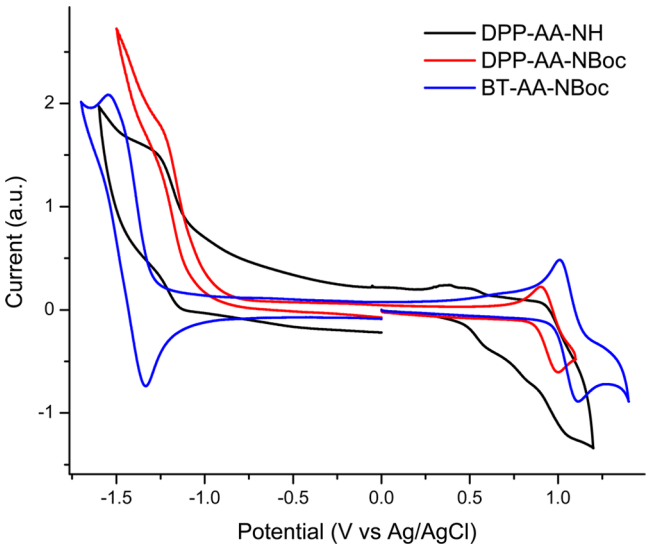

Figure 8. Cyclic voltammograms of the compounds **DPP-AA-NH** (black line), **DPP-AA-NBoc** (red line), and **BT-AA-NBoc** (blue line).

the oxidation onset for **DPP-AA-NH** 0.38 V lower than that of **DPP-AA-NBoc**, but also, **DPP-AA-NH** presents multiple redox process whereas **DPP-AA-NBoc** shows a single well-defined oxidation peak. The oxidation peak at 0.87 V vs Ag/AgCl for **DPP-AA-NBoc** can be assigned to oxidation at the **DPP** unit,[25] whereas for **DPP-AA-NH**, the first oxidation can be attributed to the *N*-H group. The multiple redox process might be assigned to the presence of trace impurities (see the ^{1}H NMR spectrum in the Supporting Information) or partial decomposition of **DPP-AA-NH**, although we do not have enough experimental evidence to reach a conclusion on the exact nature of these multiple processes. Unexpectedly, the reduction potential for **BT-AA-NBoc** is −1.3 V vs Ag/AgCl, which is quite high considering the presence of the electron-withdrawing **BT** group. This can be attributed to the poor electronic communication between the **BT** group and the anthanthramine core. This hypothesis is supported by the UV−vis spectrum (vide supra).

TPD-AA-NH and **TPD-AA-NBoc** follow the same trend with a lower oxidation potential for the secondary amine and a negligible modulation of the reduction potential (Figure 9). Quinoidal **T-AA-Imine** shows a similar (although irreversible) oxidation potential as the *N*-Boc species at 1.03 V vs Ag/AgCl, supporting the assumption that the Boc group greatly reduces the electron-donating character of the arylamine. The reduction onset at −1.01 V vs Ag/AgCl is lower by about 0.3 V compared with the anthanthramine compounds. This fairly high reduction potential indicates the weak electron-withdrawing character of the imine. This can easily be modulated by the right choice of electron-withdrawing substituent on the aniline moiety.[24]

DFT Calculations. Using the commonly used B3LYP/6-31G* model,[27] we performed DFT calculations on **TPD-AA-NH**, **TPD-AA-NBoc**, and **T-AA-Imine** as representative examples to determine the optimized geometrical structure and the distribution of the HOMO and LUMO frontier

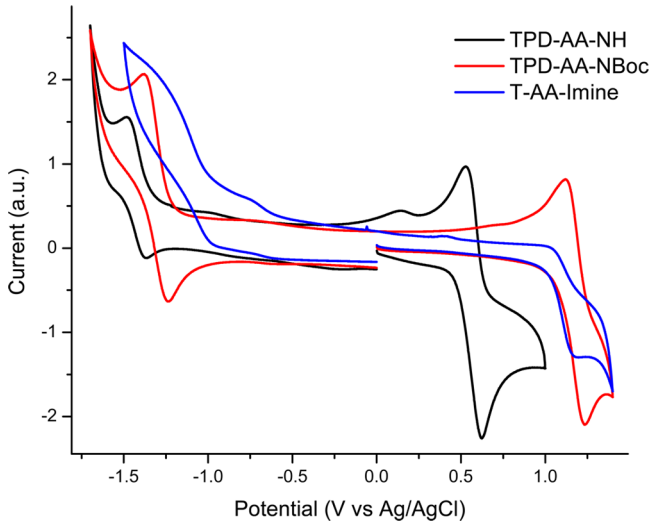

Figure 9. Cyclic voltammograms of the compounds **TPD-AA-NH** (black line), **TPD-AA-NBoc** (red line), and **T-AA-Imine** (blue line).

orbitals. For **TPD-AA-NH,** the HOMO orbital is more strongly delocalized over the *N*-phenyl moieties than for the *N*-Boc analogue and contributes to the higher HOMO energies for the *N*-H compounds (Figure 10). The difference between the HOMO energies of the *N*-Boc and *N*-H compounds was accurately calculated to be 0.57 eV, which is close to the experimental value of 0.59 eV. The LUMO was expected to be localized over the **TPD** unit because of its electron-withdrawing character, but for both compounds, the delocalization of the LUMO beyond the anthanthramine core is quite limited. Interestingly, in case of **TPD-AA-NH**, we observed a short carbonyl−HN distance of 2.52 Å, indicative of weak hydrogen bonding, as depicted in Figure 11.[28] A reduced dihedral angle of 33° between the anthanthramine and TPD planes is observed for **TPD-AA-NH**, whereas **TPD-AA-NBoc** presents a dihedral angle of 52°. Therefore, it appears that the hydrogen bonding forces planarization by approximately 20°, but the rather large dihedral angle still present limits the effective conjugation. The difference in the dihedral angles can be partly responsible for the difference in the absorption spectra for **TPD-AA-NH** and **TPD-AA-NBoc** in solution (Figure 3).

For compound **T-AA-Imine**, we chose to model the *anti* isomer because it should be less sterically hindered and therefore most favored. The HOMO for **T-AA-Imine** appears to be highly delocalized over the whole molecule even though the large calculated dihedral angle of 52° between the dihydroanthanthrene and thiophene planes was expected to limit the conjugation (Figure 12). The imine moiety allows for a nearly planar configuration with a LUMO largely delocalized over the dihydroanthanthrene core and the imine nitrogen atom.

Two important factors that influence the band gap of π-conjugated materials are the resonance energy and the planarity, which are closely connected.[16] Although in the present system a donor−acceptor approach was used to modulate the band gap of the materials, the resulting effect was rather limited. This can be attributed to structural and electronic factors. First, the torsion angle between the polycyclic core and the thiophene unit is about 30° because of steric hindrance. This value is quite far from the ideal fully planar value of 0° and limits the effective conjugation. A simple

dx.doi.org/10.1021/jo402313c | J. Org. Chem. 2013, 78, 12769−12778

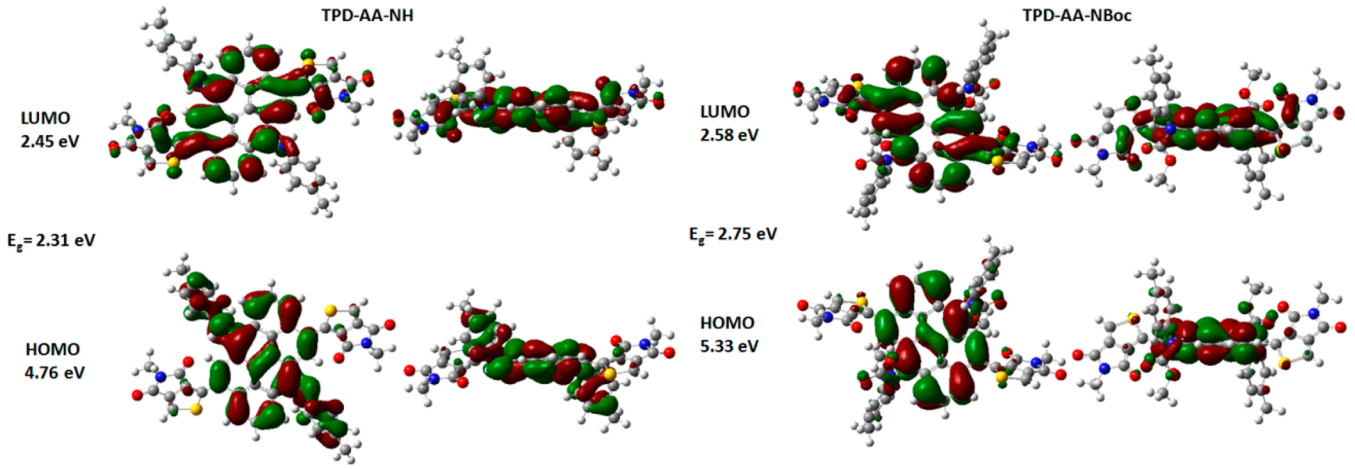

Figure 10. Calculated frontier orbitals for **TPD-AA-NH** and **TPD-AA-NBoc**.

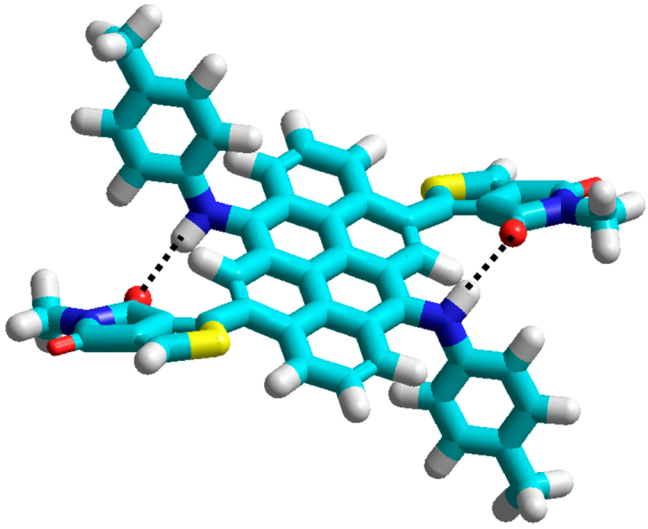

Figure 11. DFT-optimized structure of **TPD-AA-NH** with hydrogen bonds depicted as black dashed lines.

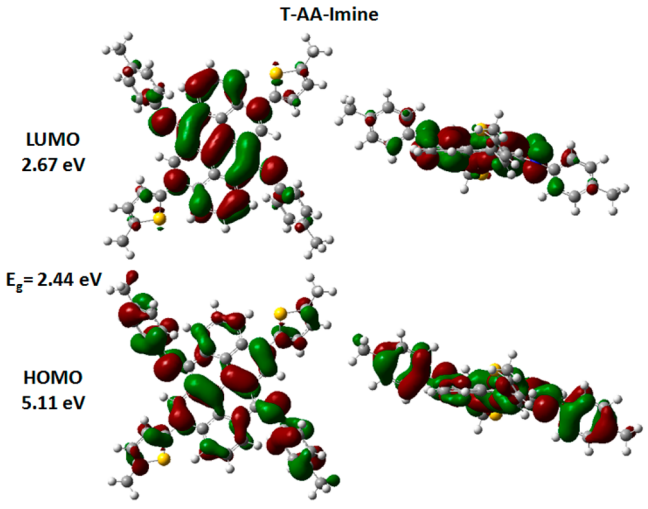

Figure 12. Calculated frontier orbitals for **T-AA-Imine**.

solution to overcome this limitation would be the use of unhindered acetylenic or ethylenic linkers. Furthermore, an aromatic system must overcome its aromatization energy to adopt the quinoidal mesomeric form and the conjugated alternation of single and double bonds. Four possible mesomeric structures of the polycyclic aromatic anthanthrene are presented in Figure 13. According to Clar's aromatic π-sextet rule and NCIS calculations,[29] the **B** and **C** rings are significantly more aromatic than the **A** ring, with **C** being the most aromatic with a NCIS value of −12.70. Therefore, the mesomeric structure **M1** should be the most favored. Hybridization to the quinoidal form **Q1** (4,10-axis) requires the dearomatization of two **C** rings and therefore has a large energetic cost. The large resonance energy of the anthanthrene therefore limits the effective conjugation along the 4,10-axis. The 6,12-axis presents a second possible pathway of conjugation with a possible mesomeric structure **Q2**, analogous to the anthanthrone and **T-AA-Imine** compounds. For **Q2**, the aromaticity in **C** is conserved, and thus, the resonance energy cost of hybridization to the quinoidal structure should be lower, possibly making the 6,12-axis a better conjugation pathway. Interestingly, the aromaticity in **C** is conserved in **Q3** with the quinoidal structure in both the 4,10- and 6,12-axis, which could make the anthanthrene core a promising structure for efficient 2D conjugated materials. More extensive theoretical calculations are currently underway to verify this hypothesis.

■ CONCLUSION

Functionalization of the 6 and 12 positions of anthanthrone derivatives with *N*-(4-octylphenyl) moieties via $TiCl_4$-mediated imine condensation afforded versatile building blocks. The dihydroanthanthrene bisimine can be obtained in a single step, and a subsequent reduction step affords the aromatic secondary diarylamine anthanthramine. *N*-Boc protection was used as a synthetic and functional strategy to control the optoelectronic and packing properties of the materials, which can be paired with facile thermal deprotection amenable to solid-state postprocessing steps. Introduction of the *N*-Boc group greatly improves the solubility while limiting the intermolecular interactions and increasing the oxidation potential by ca. 0.5 V over the *N*-H compounds. The secondary anthanthramines have lower oxidation potentials and stronger intermolecular interactions, which can be used to tune the properties of the materials and reach the lower energies desirable for photovoltaic applications. Functionalization of the 4 and 10 positions via either Suzuki or Stille cross-coupling with different electron-donating or -accepting moieties showed a very limited

dx.doi.org/10.1021/jo402313c | J. Org. Chem. 2013, 78, 12769−12778

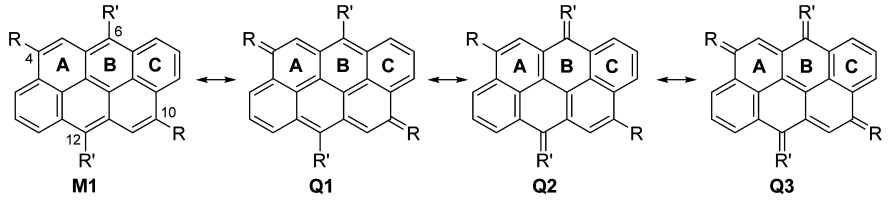

Figure 13. Mesomeric structures of anthanthrene.

modulation of the optoelectronic properties via donor−acceptor interactions in solution, whereas some modulation can be achieved in the solid state, especially with **DPP-AA-NH**. We ascribe these surprising results to the poor electronic communication between the anthanthramine core and the appended units because of the high resonance energy of the anthanthrene moiety and the torsion angle between the two units. The quinoidal structure observed in the **T-AA-Imine** compound afforded a broad absorption spectrum in the visible region and extended delocalization of the HOMO as calculated by DFT and should serve a versatile building block with tailorable electron-accepting character. Although the secondary diarylamine *N*-H groups have seldom been used in conjugated systems, they allow an additional way to control the solid-state properties and should present interesting charge-transport properties.

EXPERIMENTAL SECTION

Materials. 4,10-Dibromoanthanthrone was supplied as a courtesy by Heubach GmbH as Monolite Red 316801 product.

Electrochemical Measurements. All of the CVs were acquired employing a three-electrode BAS Epsilon potentiostat (purchased from Bioanalytical Systems). The potential was referenced to a Ag/AgCl saturated KCl electrode (purchased from Bioanalytical Systems), and Pt wires were used as the working and counter electrodes. CH_2Cl_2 with Bu_4NPF_6 (0.1 M) as the supporting electrolyte was sparged using argon for 5 min prior to electrochemical measurements. For calculation of vacuum levels, the potentials were calibrated against a ferrocene/ferrocenium external standard measured at 0.43 V versus the Ag/AgCl reference electrode.

Computational Methods. DFT calculations were carried out with the Gaussian 03 program suite at the B3LYP/6-31G* level in vacuum using the default optimization parameters. The orbital plots are reported at an isovalue of 0.02. Alkyl chains were replaced by methyl groups to shorten the calculation time.

4,10-Dibromo-*N*^{6},*N*^{12}-bis(4-octylphenyl)anthanthrene-6,12-diamine (Br-AA-NH). A dry flask under argon was charged with 1,4-diazabicyclo[2.2.2]octane (DABCO) (1.16 g, 10.34 mmol), 4-*n*-octylaniline (707 mg, 3.45 mmol), and anhydrous *o*-dichlorobenzene (30 mL) and heated to 80 °C. A solution of $TiCl_4$ in dichloromethane (3.45 mL, 3.45 mmol, 1 M) was added dropwise over 5 min, and the mixture was stirred for an additional 5 min before 4,10-dibromoanthanthrone (800 mg, 1.724 mmol) was added and the temperature was raised to 115 °C. The resulting solution was stirred vigorously at that temperature for 3 h. Once cooled to room temperature, the reaction mixture was poured into methanol (100 mL), and the precipitate was filtered off and rinsed with methanol. The crude residue (ca. 1.76 g) was suspended in $CHCl_3$ (50 mL), and HI (55% w/w in H_2O, 0.6 mL, 550 mg, 4.3 mmol) diluted in H_2O (5 mL) was added, after which the solution was stirred overnight. Methanol (30 mL) was added, and the precipitate was recovered via vacuum filtration and air-dried. The residue was dissolved in hot $CHCl_3$ (200 mL), filtered on a silica gel pad, and washed with hot $CHCl_3$. Evaporation of the filtrate afforded compound **Br-AA-NH** as an orange solid (889 mg, 61%). Mp: 255−258 °C. ^{1}H NMR (500 MHz, $CDCl_3$): δ 8.55 (dd, J = 7.5, 1.0 Hz, 2H), 8.44 (dd, J = 8.3, 1.0 Hz, 2H), 8.38 (s, 1H), 8.05 (dd, J = 8.3, 7.5 Hz, 2H), 6.93 (d, J = 8.2 Hz, 4H), 6.51−6.45 (m, 4H), 5.72 (s, 2H), 2.52−2.45 (m, 4H), 1.55−1.50 (m, 4H), 1.35−1.22 (m, 20H), 0.97−0.83 (m, 6H). ^{13}C NMR (125 MHz, $CDCl_3$): δ 145.60, 133.7, 129.3 (2C), 127.3, 126.6, 125.4, 123.8, 114.3, 35.1, 31.8, 31.7, 29.4, 29.4, 29.3, 22.7, 14.08. HRMS (APPI$^+$): calcd for $C_{50}H_{52}Br_2N_2$ 838.2497, found 838.2475 (M*)$^+$.

4,10-Dibromo-*N*^{6},*N*^{12}-bis(4-octylphenyl)-*N*^{6},*N*^{12}-bis(*tert*-butyl carbamate)anthanthrene-6,12-diamine (Br-AA-NBoc). A dry flask under argon equipped with a reflux condenser was charged with compound **1** (1.1 g, 1.31 mmol), di-*tert*-butyl dicarbonate (0.856 g, 3.92 mmol), dimethylaminopyridine (32 mg, 0.26 mmol), and anhydrous THF (5 mL) and heated to reflux for 5 h. After the solution was cooled to room temperature, CH_2Cl_2 and H_2O were added, and the aqueous layer was extracted twice with CH_2Cl_2. The organic layer was dried with $MgSO_4$, and the solvent was evaporated under reduced pressure. The crude product was purified using a silica gel chromatography column (CH_2Cl_2/hexanes 30:70 to 100:0 v/v) to afford compound **Br-AA-NBoc** as a yellow solid (925 mg, 76%). Mp: 190 °C (decomp). ^{1}H NMR (500 MHz, $CDCl_3$): δ 8.78−8.69 (m, 6H), 8.27 (t, J = 7.9 Hz, 2H), 7.38 (d, J = 8.4 Hz, 4H), 7.06 (d, J = 8.9 Hz, 4H), 2.51 (t, J = 7.7 Hz, 4H), 1.60−1.48 (m, 4H), 1.32−1.20 (m, 38H), 0.86 (t, J = 6.9 Hz, 6H). ^{13}C NMR (125 MHz, $CDCl_3$): δ 154.3, 140.4, 139.5, 132.7, 130.0, 128.7 (2C), 128.5, 128.1, 127.4, 127.1, 126.1, 125.8, 124.3, 124.1, 123.5, 121.6, 81.8, 35.3, 31.8, 31.3, 29.4, 29.3 (2C), 29.2, 28.1, 28.0, 22.6, 14.1. HRMS (APPI$^+$): calcd for $C_{60}H_{68}Br_2N_2O_4$ 1038.3540, found 1038.3546 (M*)$^+$.

4,10-Bis(pinacolatoboronic ester)-*N*^{6},*N*^{12}-bis(4-octylphenyl)-*N*^{6},*N*^{12}-bis(*tert*-butyl carbamate)anthanthrene-6,12-diamine (2). A dry flask under argon was charged with **Br-AA-NBoc** (500 mg, 0.53 mmol), bis(pinacolato)diboron (395 mg, 1.56 mmol), anhydrous potassium acetate (233 mg, 2.37 mmol), and [1,1′-bis(diphenylphosphino)ferrocene]dichloropalladium(II) (19 mg, 0.026 mmol), and the flask was flushed three times with a vacuum/argon cycle. Anhydrous 1,4-dioxane (5 mL) was added, and the reaction was heated to 110 °C for 3 h. After the mixture was cooled, MeOH (100 mL) was added, and compound **2** was obtained after filtration as a yellow solid (478 mg, 80%). Mp: 230 °C (decomp). ^{1}H NMR (500 MHz, $CDCl_3$): δ 9.17 (d, J = 7.4 Hz, 2H), 9.01 (d, J = 8.5 Hz, 2H), 8.69 (t, J = 8.0 Hz, 2H), 8.19 (td, J = 7.9, 4.5 Hz, 2H), 7.47−7.38 (m, 4H), 7.06−6.98 (m, 4H), 2.53−2.45 (m, 4H), 1.55−1.43 (m, 28H), 1.30−1.21 (m, 38H), 0.86 (t, J = 7.0 Hz, 6H). ^{13}C NMR (125 MHz, $CDCl_3$): δ 154.8, 154.7, 141.1, 139.2, 139.0, 134.8, 133.8 (2C), 133.3, 128.5, 128.4 (3C), 126.8 (2C), 126.7, 126.3, 124.5, 124.5, 124.2, 124.4, 123.0, 122.4 (2C), 84.0, 81.1, 35.4, 35.3, 31.8, 31.4 (2C), 29.4, 29.3, 29.3, 29.2, 28.1, 28.0, 25.1, 25.0 (2C), 24.9, 22.6, 14.0. HRMS (APPI$^+$): calcd for $C_{72}H_{92}B_2N_2O_8$ 1133.7076, found 1133.7069 (M*)$^+$.

4,10-(2-Thienyl)-*N*^{6},*N*^{12}-bis(4-octylphenyl)-*N*^{6},*N*^{12}-bis(*tert*-butyl carbamate)anthanthrene-6,12-diamine (T-AA-NBoc). A dry flask under argon was charged with **Br-AA-NBoc** (100 mg, 0.105 mmol), 2-tributylstannylthiophene (0.083 mL, 98 mg, 0.26 mmol), and bis(triphenylphosphine)palladium(II) dichloride (3.6 mg, 0.0053 mmol), and the flask was flushed three times with a vacuum/argon cycle. Anhydrous toluene (3 mL) was added, and the reaction mixture was heated to 100 °C overnight. After the mixture was cooled to room temperature, CH_2Cl_2 and H_2O were added, and the aqueous layer was extracted twice with CH_2Cl_2. The organic layer was dried with $MgSO_4$, and the solvent was evaporated under reduced pressure. The crude product was purified using a silica gel chromatography column (CH_2Cl_2/hexanes 30:70) to afford compound **2** as a yellow solid (77 mg, 84%). Mp: 113−117 °C. ^{1}H NMR (500 MHz, $CDCl_3$): δ 8.72 (t, J = 8.3 Hz, 2H), 8.65 (d, J = 6.9 Hz, 2H), 8.47−8.41 (m, 2H), 8.20 (t,

dx.doi.org/10.1021/jo402313c | J. Org. Chem. 2013, 78, 12769−12778

J = 6.9 Hz, 2H), 7.54−7.34 (m, 8H), 7.27 (s, 2H), 7.07−6.98 (m, 4H), 2.49 (m, 4H), 1.51 (m, 4H), 1.40−1.15 (m, 38 H), 0.83 (t, J = 6.2 Hz, 6H). ^{13}C NMR (125 MHz, $CDCl_3$): δ 154.6, 154.5, 141.5 (2C), 140.7 (2C), 139.2, 139.1, 134.3 (2C), 133.5, 130.7 (2C), 128.9 (2C), 128.6 (2C), 127.9, 127.5 (2C), 127.4, 127.4, 126.8 (2C), 126.0 (2C), 125.3, 125.2, 124.3 (2C), 124.2, 123.7, 123.5, 123.0, 123.0, 122.1, 122.0, 81.5, 81.4, 35.3, 35.3, 31.8, 31.4, 29.4, 29.3, 29.2 (2C), 28.1, 22.6, 14.1. HRMS (APPI$^+$): calcd for $C_{68}H_{74}N_2O_4S_2$ 1046.5085, found 1046.5083 $(M^*)^+$.

4-(5-Bromothiophen-2-yl)benzo[*c*][1,2,5]thiadiazole (Br-BT). A dry flask under argon was charged with 4-thienyl-2,1,3-benzothiadiazole (245 mg, 1.14 mmol) and $CHCl_3$ (5 mL), and the reaction vessel was kept in the dark using aluminum foil. *N*-Bromosuccinimide (241 mg, 1.36 mmol) was added in three portions over 5 min. After 4 h, H_2O and CH_2Cl_2 were added, and the organic layer was washed three times with H_2O, dried with $MgSO_4$, and evaporated under reduced pressure. Recrystallization in MeOH in the freezer (ca. −15 °C) afforded **Br-BT** as a pale-yellow solid (285 mg, 85% yield). Mp: 113−116 °C. ^{1}H NMR (500 MHz, $CDCl_3$): 7.91 (d, J = 8.3 Hz, 1H), 7.79−7.71 (m, 2H), 7.58 (t, J = 7.85 Hz, 1H), 6.89 (d, J = 2.7 Hz, 1H). ^{13}C NMR (125 MHz, $CDCl_3$): 155.3, 151.8, 140.6, 130.6, 129.5, 127.5, 126.6, 124.8, 120.4, 114.5. HRMS (APPI$^+$): calcd for $C_{10}H_5BrN_2S_2$ 295.9078, found 295.9088 $(M^*)^+$.

General Procedure for Suzuki Coupling. A dry flask under argon was charged with bis(boronate) **3** (100 mg, 0.088 mmol), aryl bromide (0.22 mmol, 2.5 equiv), K_2CO_3 (122 mg, 0.88 mmol), tetrabutylammonium bromide (28.0 mg, 0.088 mmol), and bis(triphenylphosphine)palladium(II) dichloride (3.6 mg, 0.0051 mmol), and the flask was flushed three times with a vacuum/argon cycle. Toluene (3 mL) and H_2O (1 mL) were added successively, and the reaction mixture was heated to 100 °C overnight. Once the mixture was cooled to room temperature, CH_2Cl_2 and H_2O were added, and the aqueous layer was extracted twice with CH_2Cl_2. The organic layer was dried with $MgSO_4$, and the solvent was evaporated under reduced pressure. Unless otherwise specified, the crude product was purified using a silica gel chromatography column (CH_2Cl_2/AcOEt 100:0 to 99:1) to afford the corresponding compound.

4,10-(2,5-Dioctyl-3,6-bis(thiophen-2-yl)pyrrolo[3,4-*c*]-pyrrole-1,4(2*H*,5*H*)-dione)-*N*^{6},*N*^{12}-bis(4-octylphenyl)-*N*^{6},*N*^{12}-bis-(*tert*-butyl carbamate)anthanthrene-6,12-diamine (DPP-AA-NBoc). This compound was prepared according to the general procedure for Suzuki coupling with **DPP-Br** (133 mg, 0.22 mmol), and purification by silica gel chromatography afforded **DPP-AA-NBoc** as two different fractions, a polar isomer (69 mg) and a less polar isomer (63 mg), both of which were purple solids (132 mg, 78% yield). The ^{1}H NMR spectra of both compounds are presented in Figure S2 in the Supporting Information. Mp: 110−113 °C. ^{1}H NMR (500 MHz, $CDCl_3$): δ 8.99 (d, J = 3.5 Hz, 2H), 8.78 (d, J = 8.4 Hz, 2H), 8.70 (d, J = 8.4 Hz, 2H), 8.53 (s, 2H), 8.24 (t, J = 8 Hz, 2H), 7.66 (t, J = 6.68 Hz, 4H), 7.41 (d, J = 8.78 Hz, 4H), 7.31 (t, J = 4.5 Hz, 2H), 7.06 (d, J = 8.8 Hz, 4H), 4.21−4.09 (m, 8H), 2.50 (t, J = 8.2 Hz, 4H), 1.87−1.84 (m, 8H), 1.56−1.15 (m, 90H), 0.89 (t, J = 6.3 Hz, 6H), 0.84 (t, J = 6.3 Hz, 6H), 0.77 (t, J = 6.9 Hz, 6H). ^{13}C NMR (125 MHz, $CDCl_3$): δ 161.4 (2C), 154.4, 147.1, 140.6, 140.0, 139.7, 139.5, 136.2, 135.4, 134.2, 133.1, 130.8, 130.2, 130.1, 129.8, 129.7, 129.1, 128.6, 127.1, 125.7, 124.4, 124.2, 123.7, 123.5, 122.1, 108.0, 107.8, 81.6, 42.3 (2C), 35.3, 31.9, 31.8, 31.8, 31.3, 30.2, 30.0, 29.4, 29.3, 29.3 (2C), 29.2 (3C), 28.1, 26.9, 22.7, 22.6 (2C), 14.1 (2C), 14.0. HRMS (APPI$^+$): calcd for $C_{120}H_{146}N_6O_8S_4$ 1927.0085, found 1927.0260 $(M^*)^+$.

4,10-(2-Thienyl-5-benzo[*c*][1,2,5]thiadiazole)-*N*^{6},*N*^{12}-bis(4-octylphenyl)-*N*^{6},*N*^{12}-bis(*tert*-butyl carbamate)anthanthrene-6,12-diamine (BT-AA-NBoc). This compound was prepared according to the general procedure for Suzuki coupling with **BT-Br** (65 mg, 0.22 mmol), and purification by silica gel chromatography (CH_2Cl_2/hexanes 80:20 to 100:0) afforded **BT-AA-NBoc** as an orange solid (84 mg, 73% yield). Mp: 115−118 °C. ^{1}H NMR (500 MHz, $CDCl_3$): δ 8.83 (d, J = 6.7 Hz, 2H), 8.76 (t, J = 7.3 Hz, 2H), 8.56 (d, J = 9.1 Hz, 2H), 8.31 (s, 2H), 8.24−8.19 (m, 2H), 7.98 (t, J = 9.7 Hz, 4H), 7.68 (t, J = 7.9 Hz, 2H), 7.58 (s, 2H), 7.47−7.40 (m, 4H), 7.08−7.03 (m, 4H), 2.50 (m, 4H), 1.56−1.48 (m, 4H), 1.39−1.15 (m, 38H), 0.84−0.78 (m, 6H). ^{13}C NMR (125 MHz, $CDCl_3$): δ 155.6, 154.6 (2C), 152.2, 143.0 (2C), 140.8 (2C), 139.9 (2C), 139.4, 139.3, 134.1 (2C), 133.8, 130.5 (2C), 129.7, 129.1, 129.0 (2C), 128.7 (2C), 128.5, 128.4, 127.5 (2C), 127.4 (2C), 127.0 (2C), 125.5 (2C), 125.3, 125.2, 124.4 (2C), 124.3, 123.8, 123.7, 123.3, 123.2, 122.2, 122.1, 120.3 (2C), 81.7, 81.6, 35.4, 35.3, 31.8, 31.4, 29.4, 29.3 (2C), 29.2, 28.2, 22.6, 14.1. HRMS (APPI$^+$): calcd for $C_{80}H_{78}N_6O_4S_4$ 1314.4962, found 1314.4966 $(M^*)^+$.

4,10-(2-(5-Octylthieno[3,4-*c*]pyrrole-4,6-dione))-*N*^{6},*N*^{12}-bis-(4-octylphenyl)-*N*^{6},*N*^{12}-bis(*tert*-butyl carbamate)anthanthrene-6,12-diamine (TPD-AA-NBoc). This compound was prepared according to the general procedure for Suzuki coupling with 2-bromo-5-octylthieno[3,4-*c*]pyrrole-4,6-dione (76 mg, 0.22 mmol), and purification by silica gel chromatography afforded **TPD-AA-NBoc** as a yellow solid (96 mg, 77% yield). Mp: 140−144 °C. ^{1}H NMR (500 MHz, $CDCl_3$): δ 8.77 (t, J = 8.5 Hz, 2H), 8.55 (d, J = 7.8 H, 2H), 8.41 (d, J = 7.4 Hz, 2H), 8.23−8.17 (m, 2H), 7.97 (d, J = 3.8 Hz, 2H), 7.44−7.35 (m, 4H), 7.08−6.99 (m, 4H), 3.62 (m, 4H), 2.52−2.46 (m, 4H), 1.72−1.16 (m, 66H), 0.89−0.82 (12H). ^{13}C NMR (125 MHz, $CDCl_3$): δ 162.7, 162.3, 162.3, 154.4, 154.3, 143.2 (2C), 140.5 (2C), 139.5, 139.4, 137.3 (2C), 134.6, 134.5, 133.1, 130.0, 129.9, 129.0, 128.9, 128.8, 128.7 (2C), 128.5 (2C), 127.4, 127.3, 127.0 (2C), 126.9, 125.3, 125.2, 124.7, 124.6, 124.5 (2C), 123.9 (2C), 123.6, 122.3, 84.1, 81.8 (2C), 38.6, 36.0, 35.3, 35.3, 34.6, 34.5, 31.9, 31.8, 31.6, 31.4 (2C), 29.5 (2C), 29.3 (3C), 29.2 (3C), 29.1, 28.5, 28.1 (2C), 26.9, 25.2, 22.7 (2C), 22.6, 20.7, 18.7, 14.1. HRMS (APPI$^+$): calcd for $C_{88}H_{104}N_4O_8S_2$ 1408.7296, found 1408.7269 $(M^*)^+$.

General Procedure for *tert*-Butyl Carbamate Thermal Deprotection. The corresponding *N*-Boc-protected compound (20−40 mg) was charged at the bottom of a 10 mL round-bottom flask and heated at 200 °C for 30 min under a continuous flow of argon. Once the compound was cooled to room temperature, $CHCl_3$ was added, and the conversion was checked by TLC. In case of incomplete conversion, the solvent was evaporated and the crude product was subjected to a second round of heating at 200 °C for 30 min.

4,10-(2-Thienyl)-*N*^{6},*N*^{12}-bis(4-octylphenyl)anthanthrene-6,12-diamine (T-AA-NH). This compound was prepared from **T-AA-NBoc** (21 mg, 0.020 mmol) according to the general procedure for Boc thermal deprotection, and the crude product was triturated with CH_2Cl_2 (10 mL) to afford **T-AA-NH** as an orange solid (17 mg, 98% yield). Mp: >260 °C. ^{1}H NMR (500 MHz, $CDCl_3$): δ 8.71 (d, J = 8.0 Hz, 2H), 8.59 (d, J = 7.6 Hz, 2H), 8.49 (s, 2H), 8.06 (t, J = 6.84 Hz, 2H), 7.49 (d, J = 4.4 Hz, 2H), 7.43 (s, 2H), 6.97 (d, J = 7.4 Hz, 4H), 6.66 (d, J = 7.6 Hz, 4H), 6.31 (s, 2H), 2.50 (t, J = 6.7 Hz, 4H), 1.35−1.18 (m, 24H), 0.86 (m, 6H). The solubility proved to be too low to acquire a well-resolved ^{13}C NMR spectrum. HRMS (APPI$^+$): calcd for $C_{58}H_{59}N_2S_2$ 847.4120, found 847.4125 $(M + H)^+$.

4,10-(2,5-Dioctyl-3,6-bis(thiophen-2-yl)pyrrolo[3,4-*c*]-pyrrole-1,4(2*H*,5*H*)-dione)-*N*^{6},*N*^{12}-bis(4-octylphenyl)-anthanthrene-6,12-diamine (DPP-AA-NH). This compound was prepared from **DPP-AA-NBoc** (26 mg, 0.013 mmol) according to the general procedure for Boc thermal deprotection, and purification by silica gel chromatography ($CHCl_3$/AcOEt 100:0 to 99:1) afforded **DPP-AA-NH** as a blue solid (21 mg, 88% yield). Mp: 236−240 °C. ^{1}H NMR (500 MHz, $CDCl_3$): δ 9.11 (d, J = 3.4 Hz, 2H), 8.89 (d, J = 3.3 Hz, 2H), 8.62−8.56 (m, 4H), 8.23 (s, 2H), 8.04 (t, J = 7.3 Hz, 2H), 7.53−7.49 (m, 4H), 7.17 (t, J = 4.2 Hz, 2H), 6.97 (d, J = 8.7 Hz, 4H), 6.59 (d, J = 7.6 Hz, 4H), 5.94 (br s, 2H), 3.98−3.87 (m, 8H), 2.51 (t, J = 7.8 Hz, 4H), 1.72−1.66 (m, 8H), 1.60−1.53 (m, 4H), 1.42−1.20 (m, 60), 0.91−0.78 (m, 18H). ^{13}C NMR (125 MHz, $CDCl_3$): δ 161.0, 160.9, 147.8, 145.6, 139.3, 136.1, 135.2, 133.6, 132.3, 131.1, 130.4, 129.9 (2C), 129.7, 129.3, 129.2, 128.7, 128.4, 126.2 (2C), 125.9, 125.4, 124.3, 123.3, 123.2, 123.0, 120.4, 114.3, 114.2, 107.5, 42.3, 42.2, 35.2, 31.9 (2C), 31.8, 30.1, 29.9, 29.5 (2C), 29.4, 29.3 (2C), 27.0 (2C), 25.9, 22.7 (2C), 14.1 (3C). HRMS (APPI$^+$): calcd for $C_{110}H_{131}N_6O_4S_4$ 1727.9109, found 1727.9079 $(M + H)^+$.

4,10-(2-(5-Octylthieno[3,4-*c*]pyrrole-4,6-dione))-*N*^{6},*N*^{12}-bis-(4-octylphenyl)anthanthrene-6,12-diamine (TPD-AA-NH). This

compound was prepared from **TPD-AA-NBoc** (40 mg, 0.028 mmol) according to the general procedure for Boc thermal deprotection, and purification by silica gel chromatography ($CHCl_3$/AcOEt 100:0 to 99:1) afforded **DPP-AA-NH** as a red solid (29 mg, 85% yield). Mp: >260 °C. ^{1}H NMR (500 MHz, $CDCl_3$): δ 8.50 (s, 2H), 8.34 (d, J = 6.8 Hz, 2H), 8.18 (d, J = 7.1 Hz, 2H), 7.84 (s, 2H), 7.64 (br s, 2H), 7.00 (br s, 2H), 6.93 (d, J = 8.5 Hz, 4H), 6.65 (d, J = 8.0 Hz, 4H), 6.69 (t, J = 6.7 Hz, 4H), 2.47 (t, J = 7.8 Hz, 4H), 1.75−1.68 (m, 4H), 1.45−1.15 (m, 44H), 0.88−0.83 (m, 12H). ^{13}C NMR (125 MHz, $CDCl_3$): δ 163.0, 162.2, 145.7, 144.9, 137.1, 133.5, 133.2 (2C), 129.0, 128.5, 128.1, 127.6 (2C), 125.4, 124.6, 124.5, 124.2, 123.9, 123.1, 120.3, 114.7, 38.6, 35.1, 31.9, 31.8, 31.7, 29.4 (2C), 29.3, 29.2 (2C), 28.6, 27.0, 22.6, 14.1. HRMS (APPI$^+$): calcd for $C_{78}H_{89}N_4O_4S_2$ 1209.6320, found 1209.6320 $(M + H)^+$.

4,10-Bis(5-octylthiophen-2-yl)-*N*^{6},*N*^{12}-bis(4-octylphenyl)-dihydroanthanthrene-6,12-diimine (T-AA-Imine). A dry flask under argon was charged with 1,4-diazabicyclo[2.2.2]octane (DABCO, 97 mg, 0.86 mmol), 4-*n*-octylaniline (59 mg, 0.28 mmol), and anhydrous *o*-dichlorobenzene (5 mL). The resulting solution was heated to 80 °C, and $TiCl_4$ (54 mg, 30 μL, 0.28 mmol) was added dropwise over 5 min. The mixture was stirred for an additional 5 min before the addition of 4,10-bis(5-octyl-2-thienyl)anthanthrone (100 mg, 0.14 mmol). The temperature was raised to 115 °C, and the mixture was stirred vigorously for 3 h and then cooled to room temperature. The reaction mixture was poured into methanol (40 mL), and the precipitate was filtered off and rinsed with methanol. The crude precipitate was purified using a silica gel chromatography column (CH_2Cl_2) to afford compound **T-AA-Imine** as a red solid (88 mg, 57%). The NMR spectra are complex because of the presence of three *syn*/*anti* isomers of the imine, leading to poor resolution of the ^{13}C NMR spectra because of the many possible carbon signals. Mp: 140−143 °C. ^{1}H NMR (500 MHz, $CDCl_3$): δ 8.71−8.58 (m, 2H), 8.50−8.27 (m, 2H), 7.83−7.60 (m 2H), 7.52−7.33 (m, 1H), 7.21−7.05 (m, 6H), 6.88−6.58 (m, 7H), 2.93−2.74 (m, 4H), 2.62 (m, 4H), 1.79 (m, 8H), 1.47−1.23 (m, 40H), 0.90 (m, 12H). ^{13}C NMR (125 MHz, $CDCl_3$): δ 156.4, 155.3, 150.6, 150.0, 147.3, 138.5, 138.2, 137.3, 133.3, 133.2, 131.8, 130.7, 130.2, 129.5, 128.9, 128.0, 127.9, 127.7, 127.5, 126.7, 124.4, 124.3, 118.9, 117.1, 35.7, 35.4, 32.0, 31.9, 31.7, 30.3, 29.7, 29.6, 29.5. 29.4, 22.8 (2C), 14.2. HRMS (APPI$^+$): calcd for $C_{74}H_{89}N_2S_2$ 1069.6462, found 1069.6483 $(M + H)^+$.

■ ASSOCIATED CONTENT

Ⓢ Supporting Information

Optical characterization of compounds **T-AA-NH** and **T-AA-NBoc**; ^{1}H NMR spectra of the isomers of **DPP-AA-NBoc**; NMR characterization of all compounds; and calculated coordinates and total energies for **TPD-AA-NBoc**, **TPD-AA-NH**, and **T-AA-Imine**. This material is available free of charge via the Internet at http://pubs.acs.org.

■ AUTHOR INFORMATION

Corresponding Author

*E-mail: jean-francois.morin@chm.ulaval.ca.

Notes

The authors declare no competing financial interest.

■ ACKNOWLEDGMENTS

This work was supported by NSERC through a Discovery Grant. J.-B.G. thanks the NSERC for a Ph.D. scholarship.

■ REFERENCES

(1) Yang, Y.; Zhao, Q.; Feng, W.; Li, F. *Chem. Rev.* **2013**, *113*, 192.

(2) (a) Wang, C.; Dong, H.; Hu, W.; Liu, Y.; Zhu, D. *Chem. Rev.* **2012**, *112*, 2208. (b) Mei, J.; Diao, Y.; Appleton, A. L.; Fang, L.; Bao, Z. *J. Am. Chem. Soc.* **2013**, *135*, 6724. (c) Facchetti, A. *Chem. Mater.* **2011**, *23*, 733.

(3) Thelakkat, M. *Macromol. Mater. Eng.* **2002**, *287*, 442.

(4) Liang, M.; Chen, J. *Chem. Soc. Rev.* **2013**, *42*, 3453.

(5) Huang, Q.; Li, H. *Chin. Sci. Bull.* **2013**, *58*, 2677.

(6) Cheng, Y.-J.; Yang, S.-H.; Hsu, C.-S. *Chem. Rev.* **2009**, *109*, 5868.

(7) Glowacki, E. D.; Irimia-Vladu, M.; Bauer, S.; Sariciftci, N. S. *J. Mater. Chem. B* **2013**, *1*, 3742.

(8) Głowacki, E. D.; Irimia-Vladu, M.; Kaltenbrunner, M.; Gsiorowski, J.; White, M. S.; Monkowius, U.; Romanazzi, G.; Suranna, G. P.; Mastrorilli, P.; Sekitani, T.; Bauer, S.; Someya, T.; Torsi, L.; Sariciftci, N. S. *Adv. Mater.* **2013**, *25*, 1563.

(9) Morin, J.-F.; Leclerc, M.; Adès, D.; Siove, A. *Macromol. Rapid Commun.* **2005**, *26*, 761.

(10) Qu, S.; Tian, H. *Chem. Commun.* **2012**, *48*, 3039.

(11) Giguère, J.-B.; Verolet, Q.; Morin, J.-F. *Chem.—Eur. J.* **2013**, *19*, 372.

(12) Fudickar, W.; Linker, T. *J. Am. Chem. Soc.* **2012**, *134*, 15071.

(13) Kenny, T.; Aly, S. M.; Fortin, D.; Harvey, P. D. *Chem. Commun.* **2012**, *48*, 11543.

(14) Compound names are abbreviated as **Ar-AA-NY**, where **Ar** = substituent at the 4 and 10 positions and **Y** = amino N substituent (H or Boc).

(15) Ishiyama, T.; Murata, M.; Miyaura, N. *J. Org. Chem.* **1995**, *60*, 7508.

(16) Roncali, J. *Macromol. Rapid Commun.* **2007**, *28*, 1761.

(17) Sun, M. *Chem. Phys.* **2006**, *320*, 155.

(18) Li, Y. *Acc. Chem. Res.* **2012**, *45*, 723.

(19) Lafleur-Lambert, A.; Rondeau-Gagné, S.; Soldera, A.; Morin, J.-F. *Tetrahedron Lett.* **2011**, *52*, 5008.

(20) Berrouard, P.; Dufresne, S.; Pron, A.; Veilleux, J.; Leclerc, M. *J. Org. Chem.* **2012**, *77*, 8167.

(21) van Mullekom, H. A. M.; Vekemans, J. A. J. M.; Meijer, E. W. *Chem.—Eur. J.* **1998**, *4*, 1235.

(22) Rawal, V. H.; Jones, R. J.; Cava, M. P. *J. Org. Chem.* **1987**, *52*, 19.

(23) Edder, C.; Armstrong, P. B.; Prado, K. B.; Fréchet, J. M. J. *Chem. Commun.* **2006**, 1965.

(24) Azoulay, J. D.; Koretz, Z. A.; Wong, B. M.; Bazan, G. C. *Macromolecules* **2013**, *46*, 1337.

(25) Palai, A. K.; Cho, H.; Cho, S.; Shin, T. J.; Jang, S.; Park, S.-U.; Pyo, S. *Org. Electron.* **2013**, *14*, 1396.

(26) Würthner, F.; Kaiser, T. E.; Saha-Möller, C. R. *Angew. Chem., Int. Ed.* **2011**, *50*, 3376.

(27) Frisch, M. J.; Trucks, G. W.; Schlegel, H. B.; Scuseria, G. E.; Robb, M. A.; Cheeseman, J. R.; Montgomery, J. A., Jr.; Vreven, T.; Kudin, K. N.; Burant, J. C.; Millam, J. M.; Iyengar, S. S.; Tomasi, J.; Barone, V.; Mennucci, B.; Cossi, M.; Scalmani, G.; Rega, N.; Petersson, G. A.; Nakatsuji, H.; Hada, M.; Ehara, M.; Toyota, K.; Fukuda, R.; Hasegawa, J.; Ishida, M.; Nakajima, T.; Honda, Y.; Kitao, O.; Nakai, H.; Klene, M.; Li, X.; Knox, J. E.; Hratchian, H. P.; Cross, J. B.; Bakken, V.; Adamo, C.; Jaramillo, J.; Gomperts, R.; Stratmann, R. E.; Yazyev, O.; Austin, A. J.; Cammi, R.; Pomelli, C.; Ochterski, J. W.; Ayala, P. Y.; Morokuma, K.; Voth, G. A.; Salvador, P.; Dannenberg, J. J.; Zakrzewski, V. G.; Dapprich, S.; Daniels, A. D.; Strain, M. C.; Farkas, O.; Malick, D. K.; Rabuck, A. D.; Raghavachari, K.; Foresman, J. B.; Ortiz, J. V.; Cui, Q.; Baboul, A. G.; Clifford, S.; Cioslowski, J.; Stefanov, B. B.; Liu, G.; Liashenko, A.; Piskorz, P.; Komaromi, I.; Martin, R. L.; Fox, D. J.; Keith, T.; Al-Laham, M. A.; Peng, C. Y.; Nanayakkara, A.; Challacombe, M.; Gill, P. M. W.; Johnson, B.; Chen, W.; Wong, M. W.; Gonzalez, C.; Pople, J. A. *Gaussian 03*, revision C.02; Gaussian, Inc.: Wallingford, CT, 2004.

(28) Steed, J. W.; Atwood, J. L. *Supramolecular Chemistry*; Wiley: Chichester, U.K., 2000.

(29) Portella, G.; Poater, J.; Solà, M. *J. Phys. Org. Chem.* **2005**, *18*, 785.